forms, we expect reactions 12 and 13. If the average number

$$[Mn(NCS)_3(DMF)_3]^- + NCS^- \rightarrow [Mn(NCS)_4]^{2-} + 3DMF \quad (12)$$
(O_h → T_d)

$$[Mn(NCS)_3(DMF)]^- + NCS^- \rightarrow [Mn(NCS)_4]^{2-} + DMF \quad (13)$$
(T_d → T_d)

of solvent molecules liberated at the third and fourth steps is almost the same, similar and moderate $\Delta S°_3$ and $\Delta S°_4$ values may result. Therefore, this may apply for the Mn^{II}–NCS^- system in DMF. Such an octahedral–tetrahedral equilibrium may not be unexpected, because an octahedral–tetrahedral equilibrium has in fact been suggested for the Cd^{II}–X^- (X = Cl, Br, I) system.[50]

Acknowledgment. This work was financially supported by Grant-in-Aid for Scientific Research No. 1540503 from the Ministry of Education, Science and Culture of Japan.

(50) Ishiguro, S.; Ozutsumi, K.; Miyauchi, M.; Ohtaki, H. *Inorg. Chem.* **1989**, *28*, 3258.

Contribution from the Department of Chemistry II, Faculty of Science, and Department of Nuclear Engineering, Faculty of Engineering, Hokkaido University, Sapporo 060, Japan

One-Electron-Transfer Reactions of Molybdenum(V) and Manganese(III) Porphyrins with Solvated Electrons and Solvent Radicals in 2-Methyltetrahydrofuran[1]

T. Suzuki,[†] T. Imamura,*[,†] T. Sumiyoshi,[‡] M. Katayama,[‡] and M. Fujimoto[†]

Received August 17, 1989

The reactions of the six-coordinate molybdenum(V) tetraphenylporphyrins $Mo^{V}O(TPP)X$ (X = Br, Cl, F, NCS, N_3, OCH_3, $OC(CH_3)_3$) with solvated electrons and solvent radicals were studied pulse-radiolytically, focusing on effects of the axial ligand X on the rates. Electron-pulse irradiation of the 2-methyltetrahydrofuran (MeTHF) solution dissolving $Mo^{V}O(TPP)X$, which possess neutral charge and are almost all the same size, causes the reduction of the central molybdenum atom, yielding $Mo^{IV}O(TPP)$ at room temperature. The constrained complexes $[Mo^{IV}O(TPP)X]^-$, formed at 77 K by γ-irradiation, are not stable intermediates in the reactions at room temperature. The reduction proceeds by an outer-sphere mechanism competitively between the reactions with the solvated electron and with the MeTHF neutral radical (MeTHF•). The second-order rate constants of the reactions with the solvated electron and with MeTHF• are in the range of 10^{10} and 10^9–10^8 M^{-1} s^{-1}, respectively, and depend on the axial ligand X. The orders of the constants are NCS > Br > Cl for the reductions by the solvated electron and NCS > Br > Cl ≈ N_3 > F > OCH_3 > $OC(CH_3)_3$ for the reductions by MeTHF•. The effects of the axial ligand on the redox potentials of $Mo^{V}O(TPP)X$ were also studied electrochemically. The redox half-wave potentials of the central molybdenum atom, Mo(V)/Mo(IV), depend on the axial ligand and are in the order Br > Cl > NCS > N_3 > F > OCH_3 > $OC(CH_3)_3$. The orders of magnitude of the radiolytic reaction rate constants almost parallel the order of the anodic shift in the redox potentials of Mo(V)/Mo(IV), as suggested by the Marcus–Hush theory; i.e., the displacement of the axial ligand X mainly reflects on the redox potentials of the central molybdenum that causes the variation in the rates for these outer-sphere redox reactions. Manganese(III) porphyrin systems were also reported in comparison with the $Mo^{V}O(TPP)X$ systems.

Introduction

In the last quarter of a century, extensive kinetic studies of radiation-induced redox reactions of metal complex ions[2–6] and metalloporphyrins[7] with solvated electrons or inorganic and organic radicals have been carried out with widespread physicochemical and biochemical interests. These studies revealed that various metal ions and metalloporphyrins react with solvated electrons with rates close to the diffusion-controlled limit.

Anbar and Hart indicated a profound effect of ligand on the reactivity of metal complexes toward hydrated electrons in the order I > Cl > F > H_2O > NH_3 > CN > OH.[2] On the other hand, Marcus and Hush predicted a correlation between the rates in outer-sphere redox reactions and the rates in electrochemical reactions.[8–11] The correlation was observed for the reaction systems V^{2+}–$Co(NH_3)_5X^{2+}$ and $Cr(bpy)_3^{2+}$–$Co(NH_3)_5X^{2+}$.[12] The correlation between chemical reaction rates and redox potentials has also been observed for the reactions of zinc porphyrins with $(CH_3)_2\dot{C}O^-$ in the order Zn(TMpyP) > Zn(TAPP) > Zn(TPPS)[7b] and for the reactions of lanthanoid elements with the hydrated electron in the order Eu^{3+} > Yb^{3+} > Sm^{3+}[3] but has not been observed for the reaction systems of actinide ions.[4,5] However, in the redox reactions of metal complexes possessing the same charge and size, no systematic studies on the effects of ligands and redox potentials on rates have been reported so far. Are there really ligand effects on the rates in the outer-sphere reactions that proceed with rates close to the diffusion-controlled limit? If so, what kinds of effects are caused?

Recently, we reported that γ-ray irradiation of oxomolybdenum(V) tetraphenylporphyrins $Mo^{V}O(TPP)X$ (X = Br, Cl, F, NCS[13]) in the glassy matrix of 2-methyltetrahydrofuran

[†] Department of Chemistry II.
[‡] Department of Nuclear Engineering.

(1) Taken in part from: Suzuki, T. D.Sc. (Rigakuhakushi) Dissertation, Hokkaido University, Sapporo, Japan, 1989.
(2) Anbar, M.; Hart, E. J. *J. Phys. Chem.* **1965**, *69*, 973.
(3) Thomas, J. K.; Gordon, S.; Hart, E. J. *J. Phys. Chem.* **1964**, *68*, 1524.
(4) Sullivan, J. C.; Gordon, S.; Cohen, D.; Mulak, W.; Schmidt, K. H. *J. Phys. Chem.* **1976**, *15*, 1684.
(5) Sullivan, J. C.; Schmidt, K. H.; Morss, L. R.; Pippin, C. G.; Williams, C. *Inorg. Chem.* **1988**, *27*, 597.
(6) (a) Anbar, M. In *Advances in Chemistry Series 50*; Gould, R. F., Ed.; American Chemical Society: Washington, DC, 1965; pp 55–81. (b) Anbar, M.; Bambenek, M.; Ross, A. B. *NSRDS-NBS* **1973**, 43. (c) Buxton, G. V.; Sellers, R. M. *NSRDS-NBS* **1978**, 62. (d) Buxton, B. V. In *Advances in Inorganic and Bioinorganic Mechanisms*; Academic: London, 1984; Vol. 3, pp 131–173.
(7) For example, see: (a) Neta, P.; Grebel, V.; Levanon, H. *J. Phys. Chem.* **1981**, *85*, 2117. (b) Neta, P. *J. Phys. Chem.* **1981**, *85*, 3678. (c) Morehouse, K. M.; Neta, P. *J. Phys. Chem.* **1984**, *88*, 1575. (d) Brault, D.; Santus, R.; Land, E. J.; Swallow, A. J. *J. Phys. Chem.* **1984**, *88*, 5836. (e) Wilkins, P. C.; Wilkins, R. G. *Inorg. Chem.* **1986**, *25*, 1908. (f) Brault, D.; Neta, P. *J. Phys. Chem.* **1987**, *91*, 4156. (g) Hambright, P.; Neta, P.; Richoux, M.-C.; Abou-Gamra, Z.; Harriman, A. *J. Photochem.* **1987**, *36*, 255.
(8) Hush, N. S. *Z. Elektrochem.* **1957**, *61*, 734.
(9) Hush, N. S. *J. Chem. Phys.* **1958**, *28*, 962.
(10) Marcus, R. A. *J. Chem. Phys.* **1956**, *24*, 966, 979; **1957**, *26*, 867; **1965**, *43*, 679.
(11) Marcus, R. A. *J. Phys. Chem.* **1963**, *67*, 853.
(12) Candlin, J. P.; Halpern, J.; Trimm, D. L. *J. Am. Chem. Soc.* **1964**, *86*, 1019.

0020-1669/90/1329-1123$02.50/0

(MeTHF) at 77 K caused the reduction of the central metal atom, yielding the constrained complexes $[Mo^{IV}O(TPP)X]^-$, in which the axial ligand X was forced to be coordinated to the central molybdenum.[14]

$$Mo^{V}O(TPP)X \xrightarrow[MeTHF,\ 77\ K]{\gamma\text{-ray}} [Mo^{IV}O(TPP)X]^- \quad (1)$$

$$[Mo^{IV}O(TPP)X]^- \xrightarrow{\Delta} Mo^{IV}O(TPP) + X^- \quad (2)$$

$$Mo^{IV}O(TPP) + MeTHF \underset{\Delta}{\overset{-\Delta}{\rightleftharpoons}} Mo^{IV}O(TPP)MeTHF \quad (3)$$

The bands of the visible absorption spectra of $[Mo^{IV}O(TPP)X]^-$ depend on the ligand X and shift to longer wavelengths in the order of X = Br > Cl > NCS > F. By the warming of the matrix, $Mo^{IV}O(TPP)$ is formed, releasing the ligand X. γ-Irradiation of the MeTHF fluid solutions of $Mo^{V}O(TPP)X$ at room temperature affords $Mo^{IV}O(TPP)$ immediately.

$$Mo^{V}O(TPP)X \xrightarrow[MeTHF,\ RT]{\gamma\text{-ray}} Mo^{IV}O(TPP) + X^- \quad (4)$$

The studies of the pulse-radiolytic reactions of a series of the $Mo^{V}O(TPP)X$ complexes are expected to give an answer whether there really exist the ligand effects on the reaction rates of the metal complexes with solvated electrons or with solvent radicals, since the six-coordinate $Mo^{V}O(TPP)X$ complexes have almost the same size and charge and no extra coordination sites around the central metal atom. One more great interest is whether the constrained complexes are intermediates or not in the reduction of the central molybdenum of $Mo^{V}O(TPP)X$ in the MeTHF fluid solutions.

In this paper, radiation chemistry of oxomolybdenum(V) and manganese(III) tetraphenylporphyrins with various axial ligands is reported. The influences of the axial ligand on the reaction rates are discussed along with the chemical properties and the redox potentials of $Mo^{V}O(TPP)X$ and $Mn^{III}(TPP)X$.

Experimental Section

Materials. The complexes $Mo^{V}O(TPP)X$ (X = Br, Cl, F, NCS, N_3, OCH_3, OC_2H_5, $OC(CH_3)_3$)[15] and $Mo^{IV}O(TPP)$[16] were prepared according to the methods reported previously. $Mn^{III}(TPP)X$ was synthesized by ligand substitution of $Mn^{III}(TPP)OAc$ according to the procedure used for the corresponding iron complex[17] and recrystallized from a hexane–dichloromethane solution followed by drying in vacuo at 150 °C. MeTHF, washed with aqueous sodium hydroxide and dried over anhydrous calcium chloride followed by refluxing over metallic sodium, was fractionally distilled and stored in the vessel of a vacuum line in contact with Na–K alloy. Every MeTHF sample solution was prepared in the dark by using a glass apparatus connected to the vacuum line and was introduced into optical quartz cells through a 60-mesh frit. The cells were sealed off from the apparatus for pulse-radiolytic measurements. Dichloromethane was distilled and passed through a basic alumina column.[18] The prepurified solvent was dried over 4-Å molecular sieves and again distilled under argon immediately before use. Polarographic grade dried reagents (Nakarai), tetrabutylammonium perchlorate (TBAP), tetraethylammonium bromide (TEAB), and tetraethylammonium chloride (TEAC) were used for cyclic voltammetry without further purification.

Measurements. Electronic spectra were recorded on a Hitachi 808 spectrophotometer. For rigid solutions at 77 K, electronic spectral measurements were made with an optical quartz cell dipping in liquid nitrogen in a Dewar vessel with two optical windows. ESR spectra were measured by using a JEOL JES-FE1X spectrometer operating at 100-kHz modulation in the X band. A 500-W xenon arc lamp (Ushio Denki) was used to photobleach (>500 nm) the trapped electron produced by γ-irradiation of the MeTHF glassy matrix at 77 K.

Steady-state radiolytic experiments at room temperature and 77 K were performed by the use of a 6.7×10^{13} Bq (1.8×10^3 Ci) ^{60}Co source at a dose rate of 40 Gy (4 krad) min^{-1}. Pulse radiolysis was carried out with an electron pulse (45 MeV) from an S-band linear accelerator (Mitsubishi) installed at Hokkaido University. The half-width of the electron pulse was 10 ns. The dose used for kinetic experiments was 5 Gy/pulse determined by KSCN dosimetry.[19] The $Mn^{III}(TPP)F$ system was irradiated with a 3.6-Gy electron pulse, because of its low solubility in MeTHF. The 5-Gy dose per pulse produces ca. 1.2×10^{-6} M solvated electron and ca. 1.4×10^{-6} M MeTHF neutral radical (MeTHF•).[20] The initial concentrations of $Mo^{V}O(TPP)X$ and $Mn^{III}(TPP)X$ were adjusted in a large excess of the solvated electron and MeTHF• for kinetic measurements. The decrease in the concentrations of $Mo^{V}O(TPP)X$ and $Mn^{III}(TPP)X$ was less than 10% per 5-Gy electron-pulse irradiation. The solution was stirred continuously in a sealed quartz cell during the measurements. The ambient temperature of the cell was kept constant at 17 ± 1 °C unless otherwise specified. The optical path lengths of the quartz cells for sample solutions and for complex-free solvents were 10 and 20 mm, respectively. The optical detection system was basically the same as that designed by Hunt and Thomas.[23] Analyzing light (1-kW xenon arc lamp, Wako Denki) was chopped by a rotating disk at 25 Hz. Since $Mo^{V}O(TPP)X$ is photoreduced at room temperature,[24] a mechanical shutter was used to cut off the analyzing light during waiting time. A cutoff filter and a slit were respectively used to eliminate second-order scattering light of the analyzing light and to control the light intensity on a photomultiplier tube (Hamamatsu Photonics R928) within acceptable limits. The light passed through the monochromator (Shimadzu Bausch and Lamb 33-86-07) was detected by a photomultiplier system. The output signal from the photodetection system was digitized every 10–200 ns with a transient digitizer (Iwatsu DM 901) and was processed with an NEC PC-9801 personal computer. As the simulation curves using the first-derived rate constants disagree with the experimental curves, rate constants were searched until the least deviations were obtained by the least-squares methods using a computer iterative analysis.

Cyclic voltammetry was carried out in an atmosphere of nitrogen at 24 °C using a Tohogiken Model 2001 potentiostat with a Tohogiken Model FG02 function generator in conjunction with an X-Y recorder (Rika Denki RW-21T). A three-electrode system consisting of a working electrode (Pt wire), a counter electrode (Pt wire coated with platinum black), and a reference electrode (a saturated calomel electrode containing aqueous sodium chloride; SSCE) was used. The SSCE was connected to the sample solution through a Vycor porous glass junction and a glass capillary (Luggin capillary), avoiding the formation of $Mo^{V}O(TPP)OH$.[25,26] The Vycor glass junction and the Luggin capillary contain TBAP–dichloromethane solutions. Sample dichloromethane solutions dissolving 5.0×10^{-4} M $Mo^{V}O(TPP)X$ and 0.05 M TBAP were deaerated by bubbling nitrogen gas prior to measurements. To the sample solutions of $Mo^{V}O(TPP)Br$ and $Mo^{V}O(TPP)Cl$ were added 9.0×10^{-3} M TEAB and 9.0×10^{-3} M TEAC, respectively, to prevent the substitution of the halo ligands with perchlorate ion. Current–voltage curves were taken at a sweep rate of 100 or 200 mV s^{-1}. Half-wave potentials were determined to be the average of the cathodic and anodic peak potentials, $(E_{p,c} + E_{p,a})/2$.

Results and Discussion

Radiolysis of MeTHF. As for the radiation chemistry of MeTHF, the mechanism of the reactions has been extensively studied.[21,27-34] The generation mechanism of the trapped electron

(13) X-ray analysis confirmed that the axial ligand NCS is coordinated to the central molybdenum via the nitrogen atom. T. Imamura et al., unpublished data.
(14) Imamura, T.; Takahashi, M.; Tanaka, T.; Jin, T.; Fujimoto, M.; Sawamura, S.; Katayama, M. *Inorg. Chem.* **1984**, *23*, 3752.
(15) Imamura, T.; Numatatsu, T.; Terui, M.; Fujimoto, M. *Bull. Chem. Soc. Jpn.* **1981**, *54*, 170.
(16) Imamura, T.; Hasegawa, K.; Fujimoto, M. *Chem. Lett.* **1983**, 705.
(17) Ogoshi, H.; Watanabe, E.; Yoshida, Z.; Kincaid, J.; Nakamoto, K. *J. Am. Chem. Soc.* **1973**, *95*, 2845.
(18) Wohlleben, G. *Angew. Chem.* **1956**, *68*, 752.
(19) Fielden, E. M.; Holm, N. W. In *Manual on Radiation Dosimetry*; Holm, N. W., Berry, R. J., Eds.; Marcel Dekker: New York, 1970; p 288.
(20) The amounts were estimated from the respective *G* values of 2.6 and 3.0 for the trapped electron and MeTHF• formed by the γ-radiolysis at 77 K.[21] In fluid solutions, some part of solvated electrons thus formed may decay very rapidly before taking part in the reactions discussed in this paper.[22]
(21) Kevan, L. *Actions Chim. Biol. Radiat.* **1971**, *15*, 81.
(22) Farhataziz; Rodgers, M. A. J. *Radiation Chemistry*; VCH Publishers: New York, 1987.
(23) Hunt, J. W.; Thomas, J. K. *Radiat. Res.* **1967**, *32*, 149.
(24) Imamura, T.; Jin, T.; Suzuki, T.; Fujimoto, M. *Chem. Lett.* **1985**, 847.
(25) Imamura, T.; Tanaka, T.; Fujimoto, M. *Inorg. Chem.* **1985**, *24*, 1038.
(26) Miura, M.; Imamura, T.; Fujimoto, M. *Polyhedron* **1986**, *5*, 1621.
(27) Dainton, F. S.; Keen, J. P.; Kemp, T. J.; Salmon, G. A.; Teply, J. *Proc. Chem. Soc.* **1964**, 265.
(28) Dainton, F. S.; Salmon, G. A. *Proc. R. Soc. London* **1965**, *A285*, 319.

and MeTHF• at 77 K is summarized as shown in eqs 5–11.[21,27,34]

$$\text{MeTHF} \rightsquigarrow \text{MeTHF}^{\bullet+} + e_m^- \quad (5)$$

$$e_m^- \rightarrow e_t^- \quad (6)$$

$$\text{MeTHF}^{\bullet+} + \text{MeTHF} \rightarrow \text{MeTHFH}^+ + \text{MeTHF}^\bullet \quad (7)$$

$$\text{MeTHF} \rightsquigarrow \text{H} + \text{MeTHF}^\bullet \quad (8)$$

$$\text{H} + \text{MeTHF} \rightarrow \text{H}_2 + \text{MeTHF}^\bullet \quad (9)$$

$$\text{MeTHF}^\bullet + e_m^- \rightarrow \text{MeTHF}^- \quad (10)$$

$$e_t^- \xrightarrow{h\nu} e_m^- \quad (11)$$

In these equations, e_m^- and e_t^- represent the mobile electron and the trapped electron respectively. The trapped electron exists as the solvated electron e_s^- in a fluid solution of MeTHF at room temperature. MeTHF$^-$ has not been definitively characterized but can be suggested.[32] Two kinds of MeTHF• that have an unpaired electron at the carbon atom adjacent to the oxygen atom are produced in the fluid MeTHF by γ-irradiation.[34] Both radicals may have similar reactivity toward substrates.[35]

The transient absorption spectra illustrated in Figure 1 upon irradiations of neat MeTHF with a 110-Gy electron pulse showed the formation of the solvated electron and MeTHF•. Absorption of the solvated electron in the region of long wavelength (λ_{max} = 2150 nm)[36] almost disappears within 1 μs. The absorption spectra centered at 280 nm at 1 and 8 μs are ascribed to MeTHF•.[27] The apparent decrease in the absorbance around 280 nm at 0 μs viz. immediately after the pulse is due to the Cherenkov radiation.[37] The decay of the solvated electron in neat MeTHF obeyed first-order kinetics for the dose and the time range used in this investigation. The value of the first-order rate constant, k^e_q, for the decay increased linearly with dose from 20 to 110 Gy and obeyed the equation of $k^e_q = (1.8 \times 10^4[\text{dose}]/\text{Gy} + 6.6 \times 10^5)$ s^{-1}.[38] However, at the dose lower than 20 Gy, k^e_q was hardly estimated because of a small absorbance change. If the linearity holds to the dose region lower than 20 Gy, k^e_q at 5 Gy is estimated to be ca. 7.5×10^5 s^{-1} and the value corresponds to a half-life of 1 μs. Disappearance of 95% of the solvated electrons requires about 4.3 μs.

The yield of MeTHF• was proportional to dose in the range 40–160 Gy. The decay curves for the dose range obeyed second-order kinetics, and the value of the rate constant was evaluated to be $k^R_q = (6 \pm 1) \times 10^6$ ϵl s^{-1}, where ε and l stand for the molar absorption coefficient of MeTHF• at 290 nm and the optical path length of the solution, respectively. The value is very close to that reported by Dainton et al., which is 6.4×10^6 ϵl s^{-1} at 270 nm and 20 °C.[27] The half-life in the decay of MeTHF• increases linearly with $[\text{dose}]^{-1}$ or $[\text{abs}]^{-1}$ in the 40–160-Gy dose. However, at pulse dose significantly lower than 40 Gy, the half-life plot deviates from the linearity and the decay curve of MeTHF• conforms somewhat more closely to a first-order rate law. At low concentrations of MeTHF•, the bimolecular reaction (MeTHF• + MeTHF•) may not occur with an appreciable rate. The half-life of MeTHF• estimated at 5-Gy electron pulse is 60–100 μs.

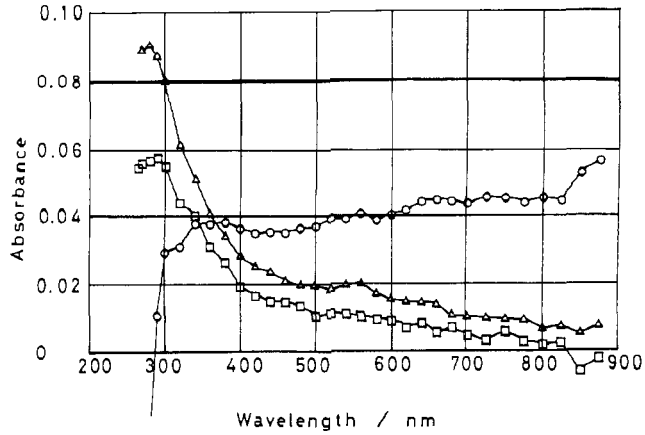

Figure 1. Transient absorption spectra after irradiation of neat MeTHF with 110-Gy electron pulse at 17 °C: (○) immediately after the pulse; (△) at 1 μs; (□) at 8 μs.

Steady-State Radiolysis. The Soret band of the absorption spectrum of $Mo^{V}O(TPP)NCS$ at 492 nm at room temperature splits into two bands at 496 and 512 nm in the glassy matrix of MeTHF at 77 K. γ-Irradiation of the $Mo^{V}O(TPP)NCS$ solution with 7×10^3 Gy at 77 K, followed by photobleaching of the trapped electron, decreased about 60% of initial absorbances of these bands with concomitant appearance of a new band at 448 nm due to the constrained complex $[Mo^{IV}O(TPP)NCS]^-$. The reducing agent to form the constrained complex is the mobile electron. As the glassy matrix was warmed to room temperature, the remaining $Mo^{V}O(TPP)NCS$ was reduced by some reducing agents other than the mobile electron or the solvated electron, affording additional $Mo^{IV}O(TPP)$. ESR measurements also confirmed the presence of other reducing agents. The central metal Mo(V) of the complex is of paramagnetic d^1 configuration. The ESR spectrum of $Mo^{V}O(TPP)NCS$ in a MeTHF glassy matrix at 77 K consists of a strong central line ($g_\perp$ = 1.963) due to ^{94,96,98,100}Mo nuclei (I = 0; natural abundance ca. 75%). γ-Irradiation of the complex solution at 77 K followed by photobleaching produced MeTHF• showing an ESR signal with seven lines at $g \approx 2$[21,28,29,32] and decreased simultaneously the height of the signal at g = 1.963 by forming $[Mo^{IV}O(TPP)NCS]^-$. The constrained complex takes a diamagnetic d^2 configuration. As the sample solution was softened and subsequently refrozen at 77 K, the ESR signal due to the remaining $Mo^{V}O(TPP)NCS$ further diminished with the disappearance of the signal based on MeTHF• even though there was an absence of the solvated electron. Other complexes $Mo^{V}O(TPP)X$ (X = Br, Cl, F, N_3, OCH_3, OC_2H_5, $OC(CH_3)_3$) were also reduced similarly. γ-Irradiation of $Mn^{III}(TPP)X$ in MeTHF causes the reduction of the central manganese atom to yield $Mn^{II}(TPP)$ at room temperature and a constrained complex $[Mn^{II}(TPP)X]^-$ at 77 K.[39,40]

In the radiolytic mechanism of MeTHF solution, candidates for the reducing species other than the mobile electron or the solvated electron are H, MeTHF$^-$, and MeTHF•. However for at least the reaction system with a low-dose irradiation, H and MeTHF$^-$ should be rejected as reducing agents by the following reasons. Atomic hydrogen reacts so fast with MeTHF as not to be detected by the ESR measurements of irradiated MeTHF at 77 K.[28] The amount of the solvated electron formed immediately after the electron-pulse irradiation of neat MeTHF increases linearly with dose up to 65 Gy. This indicates the absence of the reaction of eq 10 between MeTHF• and the solvated electron to form MeTHF$^-$ at low-dose irradiations. MeTHF• must be another reducing agent besides the solvated electron under the experimental conditions. Similar reductions have been observed on warming the rigid matrices of the reaction systems containing $FeCl_3$[27,28] or $Co^{III}(TPP)Cl$.[41] Tetracyanoethylene (TCNE) is also reduced

(29) Smith, D. R.; Pieroni, J. J. *Can. J. Chem.* **1965**, *43*, 876.
(30) Hamill, W. H. In *Radical Ions*; Kaiser, E. T., Kevan, L., Eds.; Wiley: New York, 1968; p 321.
(31) Lin, D. P.; Kevan, L. *J. Chem. Phys.* **1971**, *55*, 2629.
(32) Hager, S. L.; Willard, J. E. *J. Chem. Phys.* **1975**, *63*, 942.
(33) Dismukes, G. C.; Willard, J. E. *J. Phys. Chem.* **1976**, *80*, 1435.
(34) Murabayashi, S.; Shiotani, M.; Sohma, J. *Chem. Phys. Lett.* **1977**, *48*, 80.
(35) Hoshino, M.; Arai, S.; Imamura, M. *Radiat. Phys. Chem.* **1980**, *15*, 377.
(36) Jou, F. Y.; Dorfman, L. M. *J. Chem. Phys.* **1973**, *58*, 4175.
(37) Zimek, Z.; Zagorski, Z. P. *Nukleonika* **1979**, *24*, 983.
(38) The amount of the solvated electron formed by an electron-pulse irradiation parallels the dose.
(39) Jin, T.; Suzuki, T.; Imamura, T.; Fujimoto, M. *Inorg. Chem.* **1987**, *26*, 1280.
(40) Konishi, S.; Hoshino, M.; Imamura, M. *J. Phys. Chem.* **1982**, *86*, 1412.

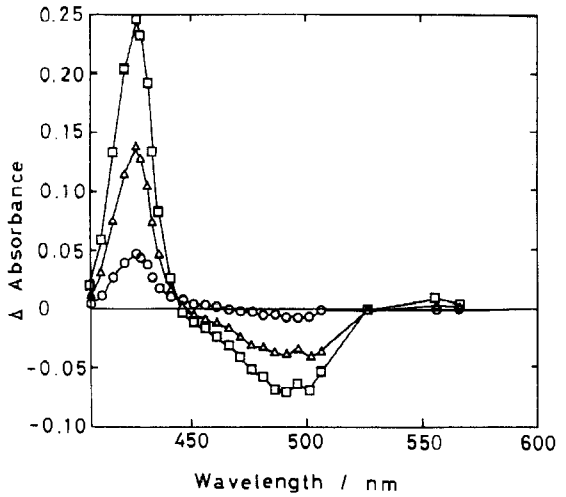

Figure 2. Differential absorption spectra upon 30-Gy pulse irradiation of 2.9×10^{-6} M $Mo^{V}O(TPP)NCS$ solution in MeTHF at 17 °C: (○) at 2 μs after the pulse; (△) at 20 μs; (□) at 160 μs.

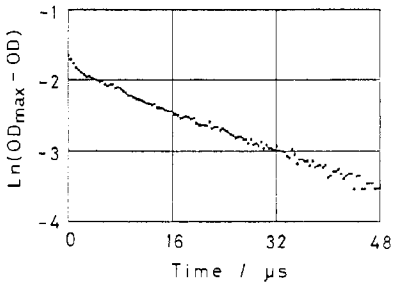

Figure 3. ln (OD_{max} − OD) as a function of time for the 1.1×10^{-5} M $Mo^{V}O(TPP)NCS$ system upon 5-Gy pulse irradiation at 17 °C. OD and OD_{max} are respectively the absorbance and the final absorbance at 420 nm of the solution.

by electron attachment and by electron transfer from MeTHF• to yield the TCNE radical anion.[35]

Pulse Radiolysis of $Mo^{V}O(TPP)X$. Figure 2 shows the transient differential absorption spectra of the $Mo^{V}O(TPP)NCS$ solution caused by the pulse radiolysis at 17 °C at 2, 20, and 160 μs after electron-pulse irradiation. The absorbance of $Mo^{V}O(TPP)NCS$ at 492 nm decreased with increase in the absorbance at 427 nm due to $Mo^{IV}O(TPP)$, and isosbestic points were clearly exhibited at 450 and 538 nm. Similar spectral changes were also observed for other $Mo^{V}O(TPP)X$ systems. These observations result in that only $Mo^{IV}O(TPP)$ is formed throughout the course of the reaction; i.e., the constrained complexes and other species such as porphyrin anion radicals are not detected.

Kinetic curves at the absorbance of 420 nm due to $Mo^{IV}O(TPP)$ with an electron-pulse irradiation of the $Mo^{V}O(TPP)NCS$ solutions are the same as those monitored at the decreasing absorbance around 492 nm due to the initial complex of $Mo^{V}O(TPP)NCS$, as the amounts of these absorbance changes are normalized. The plot of ln (OD_{max} − OD) vs time after pulse irradiation revealed that the reaction did not proceed with a simple first-order process but consisted of a fast and a slow process (Figure 3). OD_{max} and OD represent the final absorbance at 420 nm of the solution and the absorbance at appropriate time during the reaction, respectively. The logarithmic plot consists of two first-order components. These two processes correspond to the γ-irradiated reductions by the mobile electron at 77 K and by MeTHF• as the matrix is softened. The fast process was completed in 3 μs, that is, within the time of disappearance of the solvated electron, suggesting the reduction with the solvated electron. The slow process was completed in 100 μs and should be ascribed to the reduction with MeTHF•. Other $Mo^{V}O(TPP)X$ were also reduced competitively by two-reaction processes to form the same complex of $Mo^{IV}O$-(TPP). The amounts of $Mo^{IV}O(TPP)$ formed in the fast process increased with increase in the initial concentrations of $Mo^{V}O$-(TPP)X and depended upon the axial ligand X, indicating that the process also consists of the competitive reactions between the reduction of the complex and the self-disappearance of the solvated electron. The slow process is also composed of the reduction of $Mo^{V}O(TPP)X$ and the self-disappearance of MeTHF•. The Cherenkov radiation and the analyzing light caused no photoreductions; i.e., the yield of $Mo^{IV}O(TPP)$ depended only on the dose of electron pulse. The 60% decrease in dose by the slight bent of the electron beam from the analyzing light without change in the intensity of the Cherenkov radiation caused the same 60% drop of the yield of $Mo^{IV}O(TPP)$. The reaction mechanism at low-dose irradiations is proposed as follows:

Table I. Rate Constants for the Reactions of $Mo^{V}O(TPP)X$ with e_s^- and MeTHF• in MeTHF at 17 °C

complex	$k^e/10^{10}$ M^{-1} s^{-1}	$k^R/10^9$ M^{-1} s^{-1}
$Mo^{V}O(TPP)NCS$	5.1 ± 1.8	2.2 ± 0.2
$Mo^{V}O(TPP)Br$	2.2 ± 0.8	1.8 ± 0.3
$Mo^{V}O(TPP)Cl$	1.4 ± 0.8	1.3 ± 0.3
$Mo^{V}O(TPP)N_3$		1.3 ± 0.4
$Mo^{V}O(TPP)F$		0.56 ± 0.06
$Mo^{V}O(TPP)OCH_3$		0.32 ± 0.10
$Mo^{V}O(TPP)OC(CH_3)_3$		0.14 ± 0.09

$$Mo^{V}O(TPP)X + e_s^- \xrightarrow{k^e} Mo^{IV}O(TPP) + X^- \quad (12)$$

$$e_s^- \xrightarrow{k^e_q} \text{disappearance} \quad (13)$$

$$Mo^{V}O(TPP)X + MeTHF^{\bullet} \xrightarrow{k^R} Mo^{IV}O(TPP) + X^- + MeTHF^+ \quad (14)$$

$$MeTHF^{\bullet} \xrightarrow{k^R_q} \text{disappearance} \quad (15)$$

The kinetic equations under the conditions $[Mo^{V}O(TPP)X]_0 \gg [e_s^-]_0 + [MeTHF^{\bullet}]_0$, where $[Mo^{V}O(TPP)X]_0$, etc. are the initial concentrations, are

$$-d[e_s^-]/dt = k_1[e_s^-] \qquad k_1 = k^e[Mo^{V}O(TPP)X]_0 + k^e_q \quad (16)$$

or

$$[e_s^-] = [e_s^-]_0 \exp(-k_1 t) \quad (17)$$

and similarly

$$[MeTHF^{\bullet}] = [MeTHF^{\bullet}]_0 \exp(-k_2 t) \qquad k_2 = k^R[Mo^{V}O(TPP)X]_0 + k^R_q \quad (18)$$

Also

$$d[Mo^{IV}O(TPP)]/dt = k^e[Mo^{V}O(TPP)X]_0[e_s^-]_0 \exp(-k_1 t) + k^R[Mo^{V}O(TPP)X]_0[MeTHF^{\bullet}]_0 \exp(-k_2 t) \quad (19)$$

and

$$[Mo^{IV}O(TPP)] = \{k^e[Mo^{V}O(TPP)X]_0[e_s^-]_0/k_1\}[1 - \exp(-k_1 t)] + \{k^R[Mo^{V}O(TPP)X]_0[MeTHF^{\bullet}]_0/k_2\}[1 - \exp(-k_2 t)] \quad (20)$$

Figure 4 shows the linear relationship between the pseudo-first-order rate constants, k_2, and the initial concentrations for the slow process of the reduction of $Mo^{V}O(TPP)X$. The second-order rate constants, k^R, evaluated from the slopes are in the range of 10^9–10^8 M^{-1} s^{-1} and are summarized in Table I. The reaction rates decrease in the order of X = NCS > Br > Cl ≈ N_3 > F > OCH_3 > $OC(CH_3)_3$. The mean value of the intercepts is (1 ± 0.2) × 10^4 s^{-1} that is the rate of self-disappearance of MeTHF• solved as a first-order reaction. The half-life of MeTHF• is estimated to be ca. 70 μs at 17 °C.

The pseudo-first-order rate constants, k_1, were evaluated by subtracting the slow processes of the reactions from the plots of ln (OD_{max} − OD) vs time for the $Mo^{V}O(TPP)X$ (X = NCS, Br, Cl) systems. The value of k_1 increases linearly with increasing

(41) Hoshino, M.; Konishi, S.; Imamura, M. *Bull. Chem. Soc. Jpn.* **1984**, *57*, 1713.

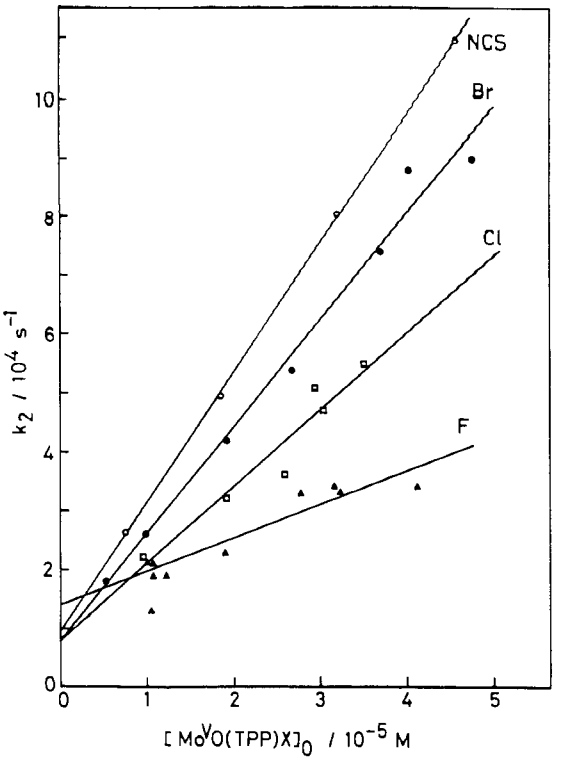

Figure 4. Dependence of k_2 on the initial concentrations of $Mo^VO(TPP)X$ (X = NCS (○), Br (●), Cl (□), F (▲)) for the reactions in MeTHF at 17 °C.

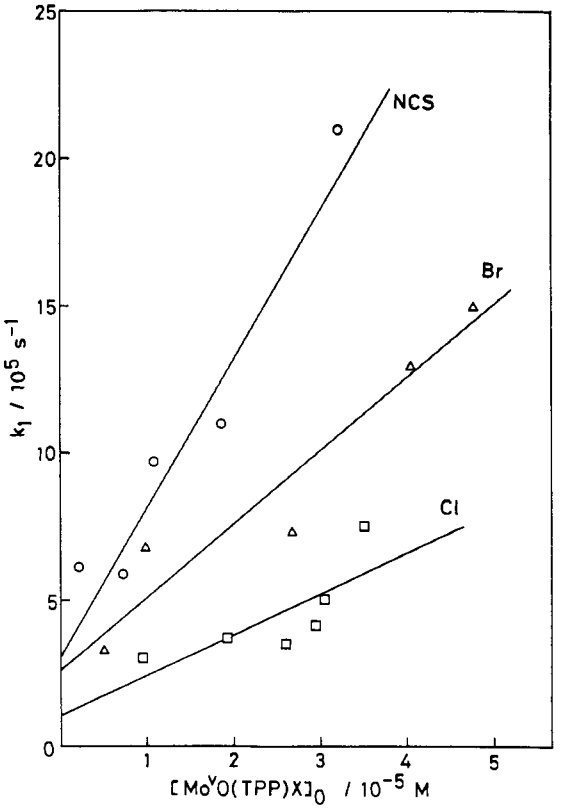

Figure 5. Dependence of k_1 on the initial concentrations of $Mo^VO(TPP)X$ (X = NCS (○), Br (△), Cl (□)) for the reactions in MeTHF at 17 °C.

initial concentrations of the sample solutions, as shown in Figure 5. For other systems of the complexes, X = F, N_3, OCH_3, $OC(CH_3)_3$, the amounts of $Mo^{IV}O(TPP)$ formed by the fast processes were too small to evaluate k_1. The second-order rate constants, k^e, derived from the slopes lie near the diffusion-controlled limit in the range of 10^{10} M^{-1} s^{-1}; nevertheless, they are influenced by the axial ligands in the order of X = NCS > Br > Cl. The order of the reaction rates is the same as that obtained for the slow reduction process of $Mo^VO(TPP)X$. The values of k_1 are higher than those of k_2 by 1 order of magnitude for the complex system possessing the same axial ligand X. The self-disappearance rate constant of the solvated electron was evaluated to be $(2 \pm 1) \times 10^5$ s^{-1} from the intercepts, which corresponds to the half-life of 2–6 μs. This value of the rate constant is close to but a little smaller than the value evaluated from the linear relationship for the complex-free neat MeTHF system with 20–110-Gy irradiations. The self-disappearance rate of the solvated electron may decrease at the low dose of 0–20 Gy.

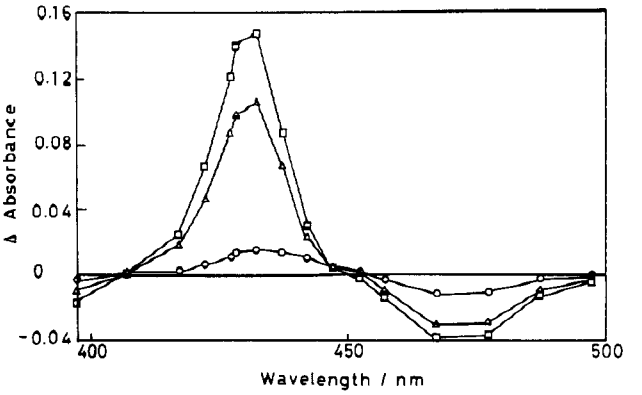

Figure 6. Differential absorption spectra upon 3.7-Gy pulse irradiation of 1.7×10^{-5} M $Mn^{III}(TPP)NCS$ solution in MeTHF at 17 °C: (○) at 2 μs after the pulse; (△) at 40 μs; (□) at 80 μs.

The amounts of $Mo^{IV}O(TPP)$ formed increased as the temperature decreased from +22 to −14 °C; i.e., the lifetimes of both the solvated electron and MeTHF• increased with lowering the temperature. However, the changes of both rates were small in the temperature range. The activation energies for the reactions of $Mo^VO(TPP)X$ (X = NCS, F) with MeTHF• are less than 3 kcal mol^{-1} (12 kJ mol^{-1}). The low energy of activation must be advantageous for the reactions with high rates.[42]

Pulse Radiolysis of $Mn^{III}(TPP)X$. Transient differential absorption spectra at room temperature of 1.7×10^{-5} M $Mn^{III}(TPP)NCS$ in MeTHF were monitored at 2, 40, and 80 μs after 3.7-Gy irradiation with electron pulse (Figure 6). The spectral change shows isosbestic points at 407 and 445 nm: the absorbance of $Mn^{III}(TPP)NCS$ at 475 nm decreased with an increasing absorbance at 430 nm due to $Mn^{II}(TPP)$ without any formation of intermediates such as the constrained complex. Similar absorption spectral changes were also observed in pulse radiolysis of other $Mn^{III}(TPP)X$ (X = Br, Cl, F) systems. Kinetic spectrophotometric curves at 430 nm and around 475 nm for the $Mn^{III}(TPP)NCS$ solution are the same, as the amounts of these absorbance changes are normalized. These curves consist of a fast and a slow component. The ratio of the amount of $Mn^{II}(TPP)$ formed in the fast process to the amount in the whole process increased from 10% to 20% as the concentration of the sample solution increased from 8.8×10^{-6} to 5.1×10^{-5} M. These results suggest that $Mn^{III}(TPP)NCS$ is reduced competitively by the reducing agents, the solvated electron e_s^-, and MeTHF•. Similar results were also observed for the pulse radiolysis of $Mn^{III}(TPP)X$ (X = Br, Cl, F). The reaction mechanism is the same as the proposed one for the $Mo^VO(TPP)X$ systems. The absorbance change in the fast process is too small to evaluate rate constants.[43] The slow process obeys first-order rate law. Apparent pseudo-first-order rate constants, k^R_{obsd}, for the slow process of the reactions with MeTHF• depend on the concentrations of the sample solutions, as shown in Figure 7. A linear relationship holds between k^R_{obsd} and the concentration for each complex solution. The second-order rate constants, k^R, evaluated from the slopes are in the range 10^8 M^{-1} s^{-1} and are affected by axial ligands in the order NCS > Br

(42) Kochi, J. K.; Subramanian, R. V. *J. Am. Chem. Soc.* **1965**, *87*, 4855.
(43) The second-order rate constant, k^e, in the reaction of $Mn^{III}(TPP)X$ with the solvated electron is estimated to be less than 2×10^{10} M^{-1} s^{-1} in comparison with that of the $Mo^VO(TPP)X$ system.

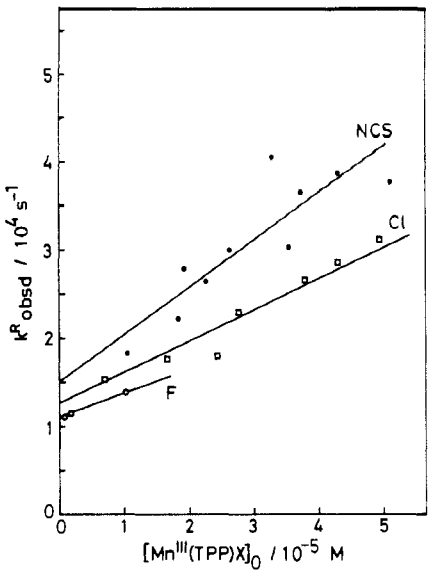

Figure 7. Dependence of k^R_{obsd} on the initial concentrations of Mn^{III}(TPP)X (X = NCS (●), Cl (□), F (○)) for the reactions in MeTHF at 17 °C. Mn^{III}(TPP)F is irradiated with a 3.6-Gy electron pulse because of its low solubility in MeTHF.

Table II. Rate Constants k^R for the Reactions of Mn^{III}(TPP)X with MeTHF• in MeTHF at 17 °C

complex	$k^R/10^8$ M^{-1} s^{-1}	$E_{1/2}/V^a$
Mn^{III}(TPP)NCS	5.1 ± 1.0	−0.25[b]
Mn^{III}(TPP)Br	4.4 ± 0.3	−0.26[b]
Mn^{III}(TPP)Cl	3.6 ± 0.3	−0.29[b]
Mn^{III}(TPP)F	2.6 ± 1.3	[c]

[a] Half-wave potentials of Mn(III)/Mn(II) in CH_2Cl_2. [b] Versus SCE.[52] [c] Reference 53.

Scheme I

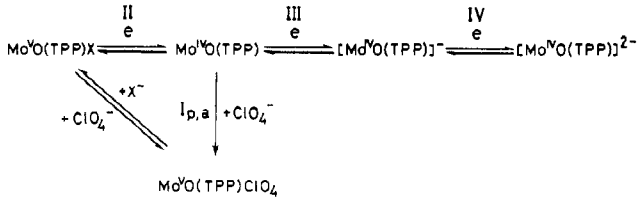

> Cl > F, as summarized in Table II. The small variation in the rate constants again suggests that the reactions proceed by an outer-sphere mechanism. Activation energy for the reduction of Mn^{III}(TPP)Cl by MeTHF• was also estimated to be less than 3 kcal mol^{-1} (12 kJ mol^{-1}) at the temperature range from +22 to −14 °C. The self-disappearance rate constant of MeTHF• (k^R_q = 1.5 × 10^4 s^{-1}) evaluated from the intercepts for the NCS, Br, and Cl systems also compares well with that in the molybdenum systems.

Electrochemistry. The redox chemistry of $Mo^{V}O(TPP)X$ in dichloromethane containing 0.05 M TBAP was investigated by means of cyclic voltammetry. The overall reaction mechanisms shown in Scheme I are very similar to those of the $Mo^{V}O(TPP)OCH_3$ system.[44,45] The half-wave potentials are presented in Table III.[46] A typical cyclic voltammogram is shown in Figure 8. In the range of potential between +0.3 and −1.7 V vs SSCE,[48]

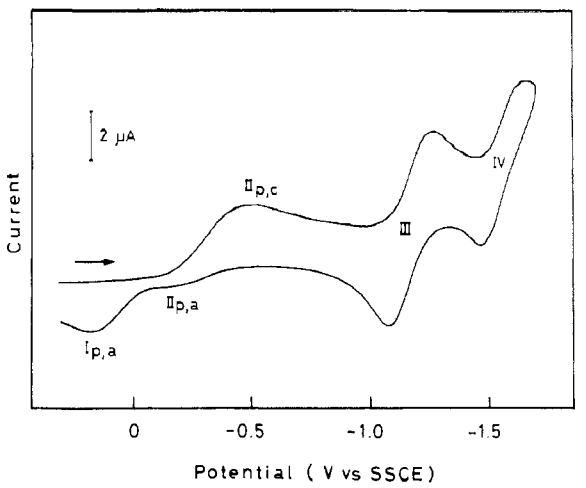

Figure 8. Cyclic voltammogram at 24 °C for the CH_2Cl_2 solution of 5 × 10^{-5} M $Mo^{V}O(TPP)NCS$ containing 0.05 M TBAP (scan rate 100 mV s^{-1}; first scan).

an anodic peak $I_{p,a}$, a cathodic peak $II_{p,c}$, a relatively small anodic peak $II_{p,a}$ coupled with $II_{p,c}$, and two well-defined redox couples, III and IV, were observed.[49] Substitution of an axial ligand resulted in drastic shifts of peaks $II_{p,c}$ and $II_{p,a}$, while peaks $I_{p,a}$, III, and IV remained almost unchanged. Half-wave potentials of II, III, and IV for the $Mo^{V}O(TPP)X$ systems possessing the same ligand X did not change at the scan rates of 100 and 200 mV s^{-1}. These cyclic voltammograms are reversible chemically, while every redox process is quasi-reversible or irreversible electrochemically; i.e., the separations of cathodic and anodic peak potentials of these waves are larger than 60 mV. This indicates that every redox process on the electrode proceeds slower than diffusion-controlled processes. In comparison with the electrochemistry of similar systems,[44,45,50] peaks $II_{p,c}$ and $II_{p,a}$ are assigned to the redox reactions between Mo(V) and Mo(IV) and peaks III and IV to successive one-electron redox processes of the porphyrin ring. Half-wave potentials $E^{II}_{1/2}$ shift to the anodic region in the order of Br > Cl > NCS > N_3 > F > OCH_3 > $OC(CH_3)_3$ and decrease with increase in separations of ΔE^{II} ($=E^{II}_{p,a} - E^{II}_{p,c}$).[51] Anodic peak $I_{p,a}$ corresponds to the oxidation of $Mo^{IV}O(TPP)$ to form $Mo^{V}O(TPP)ClO_4$. This reaction was confirmed by the absorption spectral measurements. The perchlorate ion in $Mo^{V}O(TPP)ClO_4$ formed is substituted slowly by X^- to form the starting complex $Mo^{V}O(TPP)X$. A cyclic voltammogram of the $Mo^{V}O(TPP)Br$ solution containing only 0.05 M TBAP as an electrolyte showed no peak $II_{p,c}$ of the reduction of $Mo^{V}O(TPP)Br$ to form $Mo^{IV}O(TPP)$, as shown in Figure 9a. Absorption spectral measurements showed that the $Mo^{V}O(TPP)Br$ solution without TEAB comprises a small amount of $Mo^{V}O(TPP)Br$ and a large amount of $Mo^{V}O(TPP)ClO_4$. The electrochemical reduction of the $Mo^{V}O(TPP)Br$ system proceeds at the peak $I_{p,c}$ feasibly via $Mo^{V}O(TPP)ClO_4$ supplied by the ligand substitution of $Mo^{V}O(TPP)Br$. By the addition of TEAB to the system, peak $II_{p,c}$ was observed; i.e., the reduction of molybdenum(V) occurs in $Mo^{V}O(TPP)Br$. The solution systems of $Mo^{V}O(TPP)F$ and $Mo^{V}O(TPP)OC(CH_3)_3$ in which axial ligands coordinate strongly to the central atoms have a small $I_{p,a}$ peak and a large $II_{p,a}$ peak. The $II_{p,a}$ peak is the process of the oxidation of Mo(IV) to $Mo^{V}O(TPP)F$ or $Mo^{V}O(TPP)OC(CH_3)_3$. F and $OC(CH_3)_3$ anions recombine more easily with central molybdenum than ClO_4 anions

(44) Matsuda, Y.; Yamada, S.; Murakami, Y. *Inorg. Chem.* **1981**, *20*, 2239.
(45) Kadish, K. M.; Malinski, T.; Ledon, H. *Inorg. Chem.* **1982**, *21*, 2982.
(46) The values of redox potentials for $Mo^{V}O(TPP)Cl$ reported elsewhere[44] are partially consistent with the results of this work. However, the half-wave reduction potential $E_{1/2}^{red}$ of Mo(V)/Mo(IV) evaluated to be −0.06 V vs SCE is extremely high compared to a series of our data obtained under almost the same experimental conditions. The electrochemical redox process of $Mo^{V}O(TPP)NCS$ reported[47] is treated erroneously. $Mo^{V}O(TPP)NCS$ exists as $[Mo^{V}O(TPP)Me_2SO]^+NCS^-$ in Me_2SO.[25]
(47) Topich, J.; Berger, N. *Inorg. Chim. Acta* **1982**, *65*, 131.
(48) SSCE/SCE = −0.0052 V at 25 °C. *Kagaku Binran, Kiso-hen*, 3rd ed.; The Chemical Society of Japan, Ed.; Maruzen: Tokyo, 1984; Vol. 2, p 480.
(49) Peak IV reported for the $Mo^{V}O(TPP)OCH_3$ system[45] was not observed for the present systems. Peak IV in this text corresponds to peak V in that reported system.
(50) Malinski, T.; Hanley, P. M.; Kadish, K. M. *Inorg. Chem.* **1986**, *25*, 3229.
(51) The order is the same as that of the red-shift of Soret bands in their electronic spectra[15] and is reverse that of the bond strength between the central molybdenum(V) and axial halo ligand (X = Br, Cl, F).[25]

Table III. Half-Wave and Peak Potentials (V vs SSCE) for 5×10^{-4} M $Mo^{V}O(TPP)X$ in 0.05 M TBAP–Dichloromethane Solution[a]

complex	$E^{I}_{p,a}$	$E^{I}_{1/2}$	$E^{I}_{p,c}$	$E^{II}_{p,a}$	$E^{II}_{1/2}$	$E^{II}_{p,c}$	$E^{III}_{1/2}$	$E^{IV}_{1/2}$
$Mo^{V}O(TPP)ClO_4$[b]		0.02					−1.13	−1.48
$Mo^{V}O(TPP)Br$	0.2	0.1	0.06				−1.06	−1.44
$Mo^{V}O(TPP)Br$[c]	0.1			−0.10[f]	−0.18	−0.26	−1.15	−1.48
$Mo^{V}O(TPP)Cl$[d]	0.1			−0.16	−0.26	−0.35	−1.16	−1.46
$Mo^{V}O(TPP)NCS$	0.2			−0.21	−0.36	−0.50	−1.17	−1.55
$Mo^{V}O(TPP)N_3$	0.2			−0.28	−0.44	−0.59	−1.16	−1.53
$Mo^{V}O(TPP)F$	0.2			−0.46	−0.63	−0.78	−1.19	−1.54
$Mo^{V}O(TPP)OCH_3$[e]		0.02			−0.74[g]	−0.89	−1.15	−1.50
$Mo^{V}O(TPP)OC(CH_3)_3$	0.2			−0.57	−0.80	−1.02	−1.09	−1.45

[a] All values are for single-scan measurements with a scan rate of 0.1 V/s at 24 °C. [b] Versus SCE obtained in 0.1 M TBAP solution at a rotating disk electrode.[50] [c] 9.0×10^{-3} M TEAB added. [d] 9.0×10^{-3} M TEAC added. [e] Versus SCE.[45] [f] Obtained from a linear relationship between $E^{II}_{p,c}$ and ΔE^{II} ($=E^{II}_{p,a} - E^{II}_{p,c}$) observed in this work. [g] Versus SCE.[44]

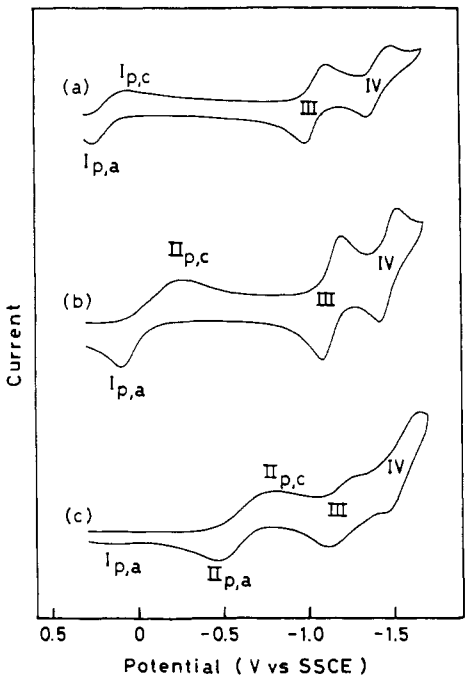

Figure 9. Cyclic voltammograms at 24 °C for the CH_2Cl_2 solutions of 5×10^{-5} M $Mo^{V}O(TPP)Br$ (a), 5×10^{-5} M $Mo^{V}O(TPP)Br$ containing 9.0×10^{-3} M TEAB (b), and 5×10^{-5} M $Mo^{V}O(TPP)F$ (c) (scan rate 100 mV s^{-1}; first scan). The solutions a, b, and c contain 0.05 M TBAP.

when $Mo^{IV}O(TPP)$ is oxidized.[25] Half-wave potentials vs SCE of the Mn(III)/Mn(II) redox couples for $Mn^{III}(TPP)NCS$, $Mn^{III}(TPP)Br$, and $Mn^{III}(TPP)Cl$ in dichloromethane are −0.25, −0.26, and −0.29 V, respectively.[52]

Mechanisms of Pulse Radiolysis. The rate constants in Table I demonstrate that the reactivity of $Mo^{V}O(TPP)X$ complexes toward the solvated electron is parallel to their reactivity toward MeTHF•. These reactions must be outer-sphere electron-transfer reactions, because these reactions proceed with rates close to the diffusion-controlled limit. Usually, much larger variations in rate occur for an inner-sphere reaction than for an outer-sphere one.[54] The rates in the reactions of $Mo^{V}O(TPP)X$ certainly depend on the axial ligands, but the differences are small. Furthermore, the small difference in the rates between the reaction systems of $Mo^{V}O(TPP)NCS$ and $Mo^{V}O(TPP)N_3$ with MeTHF• denies the mechanism via a bridge between the axial ligand and the reducing agents. The ligand X would be released from the central molybdenum like rolling down a steep slope of potential surface immediately after the electron acquisition of the central molybdenum from the solvated electron or MeTHF•. The Marcus–Hush theory[8-11] for outer-sphere redox reactions, which is very similar

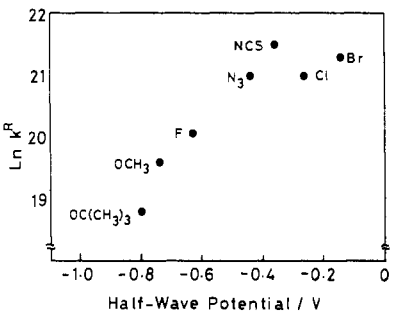

Figure 10. Plots of ln k^R vs half-wave potentials $E^{II}_{1/2}$ of Mo(V)/Mo(IV).

to the Marcus theory[55] for the reactions of the metal complexes with hydrated electrons, predicts a correlation between rates and activation free energy composed of a standard free-energy term. Figure 10 shows the plots of ln k^R vs the half-wave potentials $E^{II}_{1/2}$ of $Mo^{V}O(TPP)X$. Although there exists a small discrepancy between the order of reduction rates, NCS > Br > Cl ≈ N_3 > F > OCH_3 > $OC(CH_3)_3$, and the order of the half-wave potentials, Br > Cl > NCS > N_3 > F > OCH_3 > $OC(CH_3)_3$, the correlation between both orders is surprisingly good. In the figure, the complexes NCS, N_3, F, OCH_3, $OC(CH_3)_3$ have a linear relationship between ln k^R and the half-wave potentials. The difference of 0.4 V in the half-wave potentials between $Mo^{V}O(TPP)NCS$ and $Mo^{V}O(TPP)OC(CH_3)_3$ causes a $1^1/_2$ order of magnitude variance in the rates of the reactions with MeTHF•.

The order of the k^R values for the $Mn^{III}(TPP)X$ system, X = NCS > Br > Cl > F, is parallel to the order of the half-wave potentials. The small difference in the half-wave potentials caused only small variation in the rates. The order is also parallel to the order of the reduction rate constants of the $Mo^{V}O(TPP)X$ systems. However, the rate constants of the manganese systems are smaller than those of the systems of $Mo^{V}O(TPP)X$ possessing the same axial ligand X, despite the similarity of the half-wave potentials between these two systems, e.g., $Mn^{III}(TPP)Cl$ and $Mo^{V}O(TPP)Cl$. This trend is consistent with one general rule that a 1-equiv change in which the added electron appears in a t_{2g} orbital of the reduced product is always fast.[54] Reorganization of electrons in the molybdenum complexes may be somewhat easy as an electron is added to the d^1 configuration of the central molybdenum atom of $Mo^{V}O(TPP)X$, forming the low-spin d^2 $Mo^{IV}O(TPP)$ (electron addition to t_{2g}). In contrast with the molybdenum system, $Mn^{III}(TPP)X$ possessing a high-spin d^4 configuration forms the high-spin d^5 complex of $Mn^{II}(TPP)$ (electron addition to e_g).

We conclusively deduce that the axial ligand X in $Mo^{V}O(TPP)X$ and $Mn^{III}(TPP)X$ affects mainly the redox potential of the central molybdenum atom or manganese atom and results in the variance in the reduction rates in these outer-sphere redox reactions.

Acknowledgment. We are grateful to Dr. K. Shimazu (Department of Chemistry) for discussions on the cyclic voltammetry measurements.

(52) Kelly, S. L.; Kadish, K. M. *Inorg. Chem.* **1982**, *21*, 3631.
(53) $Mn^{III}(TPP)F$ is hardly soluble in dichloromethane,[41,49] which made impossible the measurement of half-wave potentials.
(54) Basolo, F.; Pearson, R. G. *Mechanisms of Inorganic Reactions, A Study of Metal Complexes in Solution*, 2nd ed.; Wiley: New York, 1967; Chapter 6.
(55) Marcus, R. A. *J. Chem. Phys.* **1965**, *43*, 3477.